CRYSTAL GROWTH & DESIGN

Article

Probing Crystal Nucleation of Fenoxycarb from Solution through the effect of Solvent

Jacek Zeglinski, Manuel Kuhs, K. Renuka Devi, Dikshitkumar Khamar, Avril C. Hegarty, Damien Thompson, and Åke C. Rasmuson

Cryst. Growth Des., **Just Accepted Manuscript** • DOI: 10.1021/acs.cgd.8b01387 • Publication Date (Web): 08 Mar 2019

ACS Publications

is published by the American Chemical Society. 1155 Sixteenth Street N.W., Washington, DC 20036

Probing Crystal Nucleation of Fenoxycarb from Solution through the effect of Solvent

Jacek Zeglinski[a], Manuel Kuhs[a], K. Renuka Devi[a], Dikshitkumar Khamar[a], Avril C. Hegarty[b], Damien Thompson[a,c] and Åke C. Rasmuson[a,d,*]

[a] Synthesis and Solid State Pharmaceutical Centre, Bernal Institute, Department of Chemical Sciences, University of Limerick, Limerick, V94 T9PX, Ireland

[b] MACSI, Department of Mathematics and Statistics, University of Limerick, Limerick, Ireland

[c] Department of Physics & Energy, University of Limerick, Limerick, Ireland

[d] Department of Chemical Engineering and Technology, KTH Royal Institute of Technology, Stockholm, Sweden

* Corresponding author: ake.rasmuson@ul.ie

Abstract

Induction time experiments, spectroscopic and calorimetric analysis, and molecular modelling were used to probe the influence of solvent on the crystal nucleation of fenoxycarb (FC), a medium-sized, flexible organic molecule. 800 induction times covering a range of supersaturations and crystallisation temperatures in four different solvents were measured to elucidate the relative ease of nucleation. To achieve similar induction times, the required thermodynamic driving force, RTlnS, increases in the order: ethyl acetate < toluene < ethanol < isopropanol. This is roughly matched by the order of interfacial energies calculated using the Classical Nucleation Theory. Solvent-solute interaction strengths were estimated using three methods: solvent-solute enthalpies derived from calorimetric solution enthalpies, solvent-solute interactions from Molecular Dynamics simulations, and the FTIR shifts in the carbonyl stretching corresponding to the solvent-solute interaction. The three methods gave an overall order of solvent-solute interactions increasing in the order: toluene < ethyl acetate < alcohols. Thus, with the exception of FC in toluene, it is found that the nucleation difficulty increases the stronger the solvent binds the solute.

Keywords: Crystal Nucleation, FTIR, Solution Calorimetry, Molecular Dynamics, Density Functional Theory, Statistical Analysis

1 Introduction

Crystallization is heavily used in various manufacturing industries, ranging from the production of salt to silicon wafers. The process is also used in the pharmaceutical industry, where over 90% of all pharmaceutical products contain crystalline ingredients[1], and where crystallisation is considered the single most important unit operation.[2]

However, there is insufficient understanding of crystallization, and the fundamental theory is insufficiently developed to replace empirical approaches.[3] The first step in crystallisation, nucleation, is particularly problematic. Nucleation is instrumental in determining critical parameters such as crystal morphology, size distribution and polymorphic form, but its mechanism is still debated. This fundamental lack of understanding was epitomised by the famous shortage of the HIV protease inhibitor Norvir in the 1990s due to the sudden formation of a different polymorph than the one produced for months.[4] In general, poor yields and the presence of undesirable or unpredictable polymorphs continue to plague crystallization processes at both a lab and industrial scale.[4]

Symptomatic of the unsolved nature of nucleation science is the continued use of the Classical Nucleation Theory (CNT). Developed over 100 years ago, and admitted to have several serious flaws not much later, it remains the default model for analysing experimental results. Only in recent years have alternative models been receiving wider acceptance, chief of which is the Two Step Theory.[5] The difficulty in studying nucleation arises from a combination of its stochastic nature, the nanometer size of the smallest stable nuclei (which are typically in the order of 10 to 1,000 molecules), and the great speed at which nuclei form. Thus, it is very difficult to directly observe nucleation, from both a temporal and a spatial perspective.[6]

One promising approach to understanding nucleation is studying its dependence on the solute-solvent interaction for nucleation from solution. The sensitivity of nucleation to solution chemistry has been known over 100 years.[7] According to CNT, the solid-liquid interfacial energy, γ, represents a solvent-specific contribution to the solute's thermodynamic barrier to nucleation. Thus, it is common practice to calculate γ from experimental nucleation data using CNT. A general inverse proportionality between solubility and interfacial energy has been found for aqueous solutions of inorganic salts.[8] In individual cases interfacial energies have been shown to be related to the intrinsic solvent properties such as solvent

boiling points[9] and solvent-solute interaction properties such as solvation and deformation energies.[10] Recent studies have demonstrated solvent-induced self-assembly of solute molecules prior to nucleation, as well as implicit[11] and explicit[9, 12] relationships between solution structure and polymorphic outcome.

It has previously been shown that the nucleation of salicylic acid, a small inflexible organic molecule, and risperidone, a medium-sized flexible API, may depend on the strength with which the solvent binds the molecule in solution.[13, 14] This was deduced from a relation found between nucleation difficulty and several experimental and modelled variables describing solvent-solute binding: at salicylic acid's carboxyl group, both the frequency in the Raman spectrum for the monomer and the DFT-derived 1:1 binding energy; at risperidone's carbonyl group the FTIR peak frequency; the calorimetrically-derived enthalpy of solvent-solute interaction (salicylic acid); and the DFT-derived solvation (salicylic acid) and 1:1 binding (risperidone) energy. This is also supported by results on tolbutamide[21], in which case however a particular molecular conformation formed in toluene made the nucleation more difficult than expected.

To further probe the relationship between solvent and nucleation, in the present work the nucleation of fenoxycarb (FC), a medium-sized flexible organic molecule in four different solvents is determined, and compared with various experimental and modelled thermodynamic quantities of the solvents and solutions.

Fenoxycarb (FC) has chemical formula $C_{17}H_{19}NO_4$, systematic name *2-(p-phenoxyphenoxy)ethylcarbamate,* and is shown in Figure 1. It is a flexible organic molecule that exhibits conformational isomerism in its single reported crystal form.[15] It is produced industrially as an insect growth regulator since it prevents the production of insect growth hormones.[16] Its melting temperature and enthalpy are reported as 53.16±0.14 °C and 26.98±0.04 kJ mol^{-1}, respectively.[17] It is practically insoluble in water but highly soluble in alcohols, ethyl acetate and toluene, with solubilities at 25 °C ranging from 266 to 1,660 g per kg organic solvent.[18] Recrystallization leads to platelets regardless of solvent used.[18] The relationship between the molecular structure and the resulting platelet morphology of FC has been elucidated.[19] Recrystallisation from isopropanol was found to exhibit a history of solution effect on the nucleation kinetics, whereby longer pretreatment at higher pretreatment temperatures increases the induction time.[11]

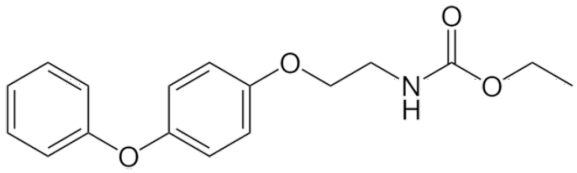

Figure 1: Molecular structure of fenoxycarb.

2 Methodology

This work includes determination of nucleation induction times of fenoxycarb in four different solvents, estimation of enthalpies of solvent–solute interaction via calorimetric determination of enthalpies of solution, evaluation of molecular interactions in solution via determination of infrared spectra, and investigation of molecular conformations and clustering by computational methods.

2.1 Induction Times

The procedure used for measuring induction times is almost identical to that reported in our previous work on this compound.[11] The differences are outlined in the Supporting Information.

2.2 Solution Calorimetry

A Precision Solution Calorimeter (TA Instruments, USA) along with Thermal Activity Monitor (TAM III) was used in semi adiabatic mode to determine the enthalpy of solution of FC in the four solvents. In each experiment, about 326-330 mg of Fenoxycarb was dissolved in 100 mL of solvent. The variation among multiple runs was ≤ 0.1 kJ mol^{-1}. The detailed experimental method is described elsewhere.[13] From the experimentally determined enthalpy of solution, $\Delta H_{solution}$, the enthalpy of solvation, $\Delta H_{solvation,}$ can be calculated provided the enthalpy of sublimation, $\Delta H_{sublimation}$ is known:

$$\Delta H_{solvation} = \Delta H_{solution} - \Delta H_{sublimation} \quad (1)$$

The enthalpy of sublimation for fenoxycarb is not reported in the literature; however the lattice energy, $E_{lattice}$, is reported: -175.9 kJ mol^{-1}.[19] From the lattice energy, the enthalpy of sublimation has been calculated as[20]:

$$\Delta H_{sublimation} = -E_{lattice} - 2RT \quad (2)$$

where R is the gas constant (J mol^{-1} K^{-1}), and T is temperature (K). Accordingly, $\Delta H_{\text{sublimation}}$ becomes 170.9 kJ mol^{-1}.

The enthalpy of solute-solvent interaction, $\Delta H_{\text{interaction}}$ is calculated from:

$$\Delta H_{\text{interaction}} = \Delta H_{\text{solvation}} - \Delta H_{\text{cavity}} - \alpha RT^2 + RT \quad (3)$$

where ΔH_{cavity} is the enthalpy of cavity formation and α is the isobaric thermal expansion coefficient of the solvent.

In our previous work we successfully used the Scaled Particle Theory (SPT) approach to determine the enthalpy of cavity formation in a range of organic solvents for the relatively small and rigid molecule of salicylic acid.[13] However the SPT approach fails to reasonably describe the solute-solvent interaction strength of a medium-sized, flexible tolbutamide molecule in an n-propanol solution.[21] Furthermore, it is known that the SPT-estimated ΔH_{cavity} can be very sensitive to the values of solvent and solute molecule diameters, and inaccurate results may be obtained for solvents with strong, directional and non-additive interactions such as alcohols.[22] In addition, the molecules are assumed to be spherically shaped objects, which becomes a poor assumption for molecules with elongated shapes such as tolbutamide or fenoxycarb. Accordingly, in the present work an alternative method is adopted.

ΔH_{cavity} is an endothermic contribution to $\Delta H_{\text{solvation}}$, and represents the enthalpy of forming the cavity in the bulk solvent where the solute molecule is to be incorporated. The higher the strength of interaction between solvent molecules and the larger the solute molecule, the higher the work required to create the cavity. In the method used here it is assumed that the volume of the cavity to accommodate a solute molecule is the same in all solvents, and is equivalent to the volume of the solute molecule. It is also assumed that the cavity is formed by breaking solvent bonding to an extent that corresponds to the solvent bonding across a surface plane having a surface area equal to half of the surface of interaction of the solute molecule occupying that cavity. This assumption should be more valid the less spherical the

solute molecule is. Molecular dynamics (MD) simulations are used to determine this solvent-solvent interaction enthalpy per solvent molecule, and is then recalculated into a value per solute molecule using respective molecular surface areas:

$$\Delta H_{solvent\ normalized} = \frac{\Delta H_{solvent}}{A^{solvent}} \times \frac{A^{solute}}{2} \qquad (4)$$

where A^{solute} and $A^{solvent}$ are the accessible solvent surfaces (units of $Å^2$) of fenoxycarb and a solvent molecule calculated at a solvent probe radius of 1.4 Å using a visualizer module of the Materials Studio molecular modelling program. From this the enthalpy of the cavity formation is calculated by:

$$\Delta H_{\text{cavity}} \approx -\Delta H_{\text{solvent normalized}} \qquad (5)$$

For detailed account on the calculation of the enthalpy of cavity formation with the new method please refer to Supporting Information.

2.3 IR Spectroscopy

IR spectra were collected using a Mettler Toledo ReactIR 10 fitted with a silver halide probe composed of diamond composite and an MCT (mercury cadmium telluride) detector cooled with liquid nitrogen. In total, 167 scans were collected for each spectrum with a resolution of 4 cm^{-1} in the spectral region of 2000-650 cm^{-1} using iC IR software version 4.3. Solution IR spectra were collected at ambient conditions (18-20 °C) and at 40 °C. The solvent spectrum is subtracted from the solution spectra. For collection of melt spectra, the IR probe was inserted into a glass vial containing crystalline material and sealed with a tight cap. This glass vial was then kept in a copper block to minimize sublimation during heat-cool cycles (54 – 20 °C) and provide uniform heating.

2.4 Computational

Energy barriers to interconversion between the different conformational isomers were calculated with density functional theory (DFT) at selected single bonds of the FC molecule. For each of the rotational centres, a relaxed potential energy surface (PES) scan over 360º was performed. In this approach, four atoms forming a dihedral angle of interest are fixed at each step of rotation (with the step interval of 5°), while the remaining atoms are allowed to adjust their positions to reach a new energy minimum. The optimised geometries and relevant energies are calculated with a B97-D Grimme's functional,[23] which includes a long-range dispersion correction, and a 6-31G(d,p) basis set.[24] A molecule of FC, extracted from the FC crystal and optimised in vacuum, served as the starting geometry for the PES scans.

To aid interpretation of experimental infrared spectra we have calculated/predicted with DFT vibrational frequencies of relevant molecular models. Calculations were performed at the B97-D3/6-31G(d,p) level using the Gaussian 09,[25] for the isolated (gas-phase) fenoxycarb molecule, a cluster of four FC molecules, and a single FC molecule solvated respectively by four molecules of toluene, ethyl acetate, and isopropanol. We restricted our solvated areas to the two most important polar groups of the fenoxycarb molecule: C=O and N-H. We manually placed two solvent molecules at a reasonable orientation and distance from each of the polar groups of the optimised fenoxycarb molecule and then optimised the whole structure again. The reason of choosing four solvent molecules was dictated by the limitations of the DFT frequency calculations we encountered. We tried various numbers of solute : solvent molecular ratios, starting from 1:1, 1:2, etc. However, when more than four solvent molecules were used in our solvation models, the Gaussian software was not able to complete the frequency calculations, probably due to the hardware limitations (not enough memory or processing power).

Molecular dynamics (MD) simulations were employed to model both diluted and concentrated solutions of FC in ethanol (ET), isopropanol (IP), ethyl acetate (EA), and toluene (TL). Eight FC model solutions (four diluted and four concentrated) were constructed. The number of molecules in a simulation box was set to achieve comparable volumes for all the modelled solutions. To simulate diluted solutions, the following compositions were applied: 1 FC + 2000 ET, 1 FC + 1500 IP, 1 FC + 1280 EA, and 1 FC + 1200 TL. The conditions of our MD simulations for concentrated solutions were set to emulate the experimental conditions, i.e. the solution concentrations and temperatures were

similar to those of the experimental supersaturated states. The simulations were performed at the crystallization temperature of 2 ºC, and we aimed to observe how the different solvents affect cluster size, cluster shape, and chief intermolecular interactions governing growth of prenucleation clusters. The molecular compositions of the simulation cells were set according to the experimental concentrations (mole fraction, x_f) at saturation temp. as follows: 160 FC + 1848 ET (0.087 x_f), 71 FC + 1207 IP (0.059 x_f), 242 FC + 673 EA (0.360 x_f), 250 FC + 665 TL (0.376 x_f). In addition, pure solvent models were constructed, containing the same amout of solvent molecules per box, as in the diluted systems. Each model was relaxed using 1000 steps of steepest descent minimization and then brought to 25 ºC over 1 ns of dynamics. Well-equilibrated stable cubic boxes were formed of edge length 58.9 ± 1.9 Å, following 15 ns (diluted solutions) and 65-100 ns (concentrated solutions) of constant pressure (1 atm) and temperature (2 ºC) dynamics with periodic boundary conditions; four of those systems are shown in Fig. S2 (Supporting Information). Molecular Langevin dynamics were performed using the NAMD program[26] with Ewald summation used to calculate the electrostatic interactions. Solvent-solute binding energies were calculated using the NAMD energy suite of the VMD program[27] as follows: for dilute solutions and pure solvents, by selecting configurations/frames generated during 10 ns of dynamics, after the initial 5 ns of a simulation; for concentrated systems, by selecting the frames generated for 50 ns, after the initial 10 ns.

All the molecules used in the MD simulations were parametrized with Charmm General Force Field (CGenFF) v. 2b7,[28] which is dedicated for modelling drug-like molecules and covers a wide range of chemical groups present in biomolecules and drug molecules, including a large number of heterocyclic entities. The FC molecule was built by bridging with an oxygen atom two residues available in the CGenFF parameters and topology files, i.e. a biphenyl (C37) and diethylcarbamate (DECB).

3 Results

3.1 Crystal Nucleation

Nucleation induction time distributions were recorded at a combination of different supersaturation ratios, S, and nucleation temperatures, T_{cry}, in four different organic solvents (ethyl acetate, toluene, ethanol and isopropanol) and results are given in Figure 2.

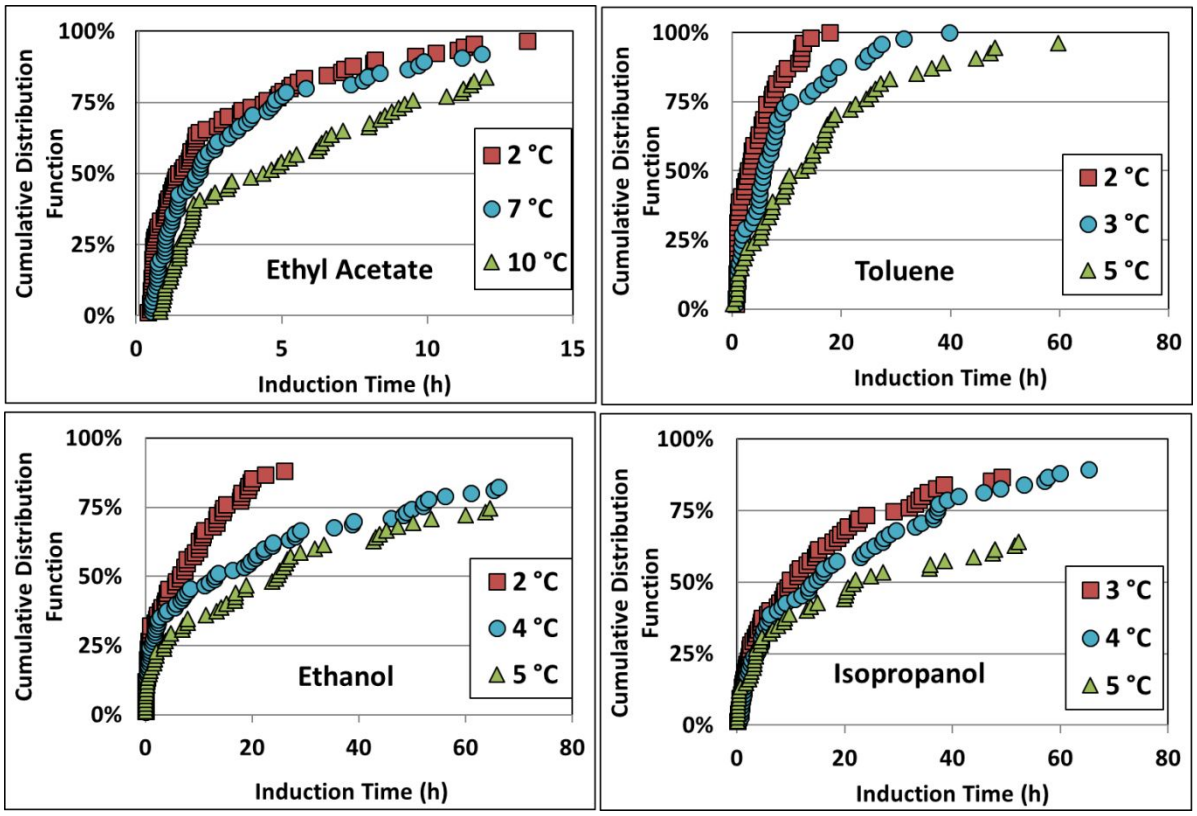

Figure 2: Induction time distributions of FC in different solvents. Temperatures are T_{cry}.

Table 1: Solutions and induction time results. $S = x/x^*$, where x is the actual mole fraction of FC in the solution, and x^* the equilibrium mole fraction at T_{cry} from Ref. 18; n is the number of induction times measured for each condition;

Solvent	T_{sat} (°C)	Mole fraction (x)	T_{cry} (°C)	Mole fraction (x^*)	S	RTlnS (kJ/mol)	n	Median t_{ind} (h)
Ethyl Acetate	15	0.360	10.0	0.290	1.24	0.51	62	4.35
			7.0	0.261	1.38	0.75	69	2.10
			2.1	0.214	1.68	1.19	87	1.45
Toluene	20	0.376	5.1	0.172	2.19	1.81	52	12.77
			3.1	0.154	2.44	2.05	48	5.73
			2.1	0.145	2.59	2.18	54	2.95
Ethanol	20	0.087	5.1	0.021	4.18	3.31	56	24.73
			4.0	0.019	4.66	3.55	74	13.12
			2.1	0.015	5.64	3.96	65	6.55
Isopropanol	20	0.059	5.1	0.013	4.58	3.52	48	21.83
			4.0	0.011	5.19	3.80	67	14.37
			3.1	0.010	5.74	4.01	65	9.86

The median induction times are plotted directly against the thermodynamic driving force of nucleation, $RT_{cry}\ln S$,[8] in Figure 3.

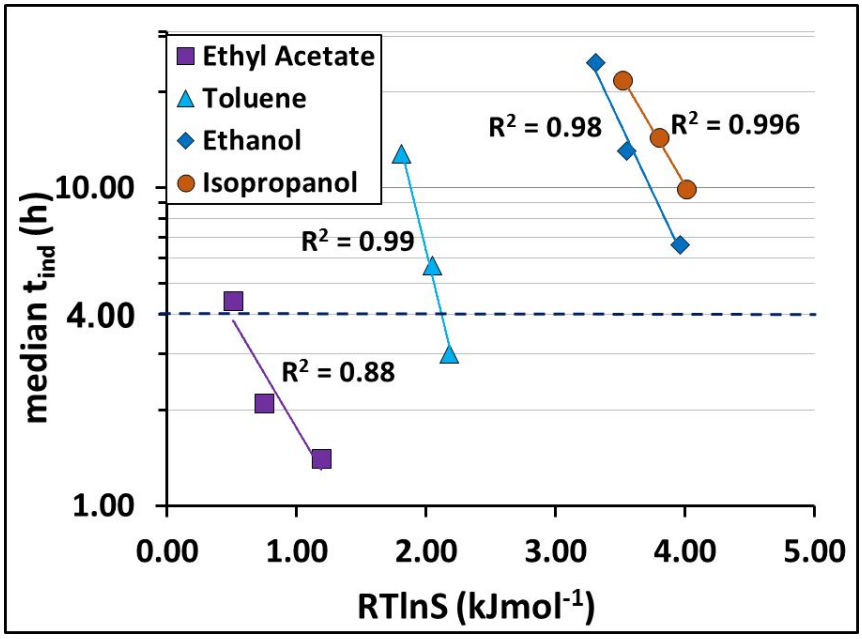

Figure 3: The relationship between median induction time and thermodynamic driving force of nucleation of FC in different solvents. Lines are guides for the eyes only.

From this plot an order of propensity for nucleation of fenoxycarb in the different solvents, called "ease of nucleation", can be established in the range of experimental induction times. In order to reach the same median induction time, the required driving force depends on the solvent. The lower the driving force the more easy the nucleation is said to be. In this work the data in the different solvents do not cross over one another in the experimental range but they do require extrapolation for a comparison to be made of the specific driving force required to reach a particular median induction time. Overall though the figure shows that in ethyl acetate solution the thermodynamic driving force required to nucleate fenoxycarb is clearly the lowest, in toluene a higher driving force is required and in the alcohols the driving force clearly has to be the highest, in isopropanol slightly higher than in ethanol.

Using the fact that behind every median value there is an induction time distribution (with at least 40 individual values) instead of using the three actual medians, through a detailed statistical analysis using survival analysis techniques (Supporting Information), it can be shown that regression lines are statistically significant for all four solvents and also that there is a significant difference between all four solvents for both slopes and intercepts, though

there is a borderline difference between the two alcohols. Survival analysis[29, 30] is a method for analysing data where the outcome variable is the time until the occurrence of an event of interest – in our case crystal nucleation. Unlike other methods e.g. standard regression, survival models incorporate information from samples for both events, those which have occurred (nucleated) and for those which have not yet occurred, to estimate the model parameters. It also allows the prediction of times for concentrations other than those actually observed. The Cox proportional hazards model[31] is the most popular model used for survival analysis and has been used in the present work. It allows the testing for differences in survival times between several groups, and adjustment for covariates may also be made.

The survival analysis has been used to estimate the survival curves for each solvent at each concentration and the Cox proportional hazards model has been used to test the significance of effects of the solvents and the driving force parameter and also to estimate the median time to nucleation. This model also allows us to predict the survival curves in solvents at different driving force values to those actually observed and so to estimate additional median times. The basis for this use of the survival analysis is that the model do fit the induction time distributions and the influence of the driving force, as is shown to be the case for the present data. Further details are given in the Supplementary Information File.

To reach the same median nucleation induction of t_{ind} = 4.0 h the required driving force, RTlnS, is 0.47 in ethyl acetate, 2.1 in toluene, 4.2 in ethanol and 4.6 kJ/mol in isopropanol (See Figure 3). As an empirical observation these values are statistically significantly correlated to solubility (R^2=0.99, p<0.01) and solvent density (R^2=0.97, p=0.01) (Supporting Information Figure S1). For further evaluation, the results are plotted according to the Classical Nucleation Theory (CNT) (Supporting Information Figure S2). From this, interfacial energies (γ) and preexponential factors (A) were calculated for each solvent (Table 2) from the slopes and intercepts, respectively, of the exponential fits of Figure S2 (Supporting Information). The absolute values of γ are of the same order of magnitude as found in other studies for similar compounds.[9, 10]

Table 2: Preexponential factors (A), interfacial energies (**γ**), the number of molecules in the critical nucleus (n*), and Gibbs free energies (ΔG*) of the critical nuclei, calculated from CNT.

Solvent	**A (m^{-3} s^{-1})**	**γ (mJ m^{-2})**	**n***	**ΔG* (kJ mol^{-1})**
Ethyl Acetate	12.79	0.92	13.1	3.31
			4.0	1.51
			1.0	0.60
Toluene	110.20	3.19	11.9	10.78
			8.2	8.44
			6.9	7.48
Ethanol	51.54	4.70	6.3	10.39
			5.1	9.08
			3.7	7.28
Isopropanol	18.45	4.46	4.5	7.84
			3.5	6.69
			3.0	5.97

As is shown in Figure 4, there is a statistically significant correlation (R^2=0.94, p=0.03) between the driving force to reach an induction time of 4.0 hours and the interfacial energy determined within CNT. The order of the alcohols is reversed, but they are quite close.

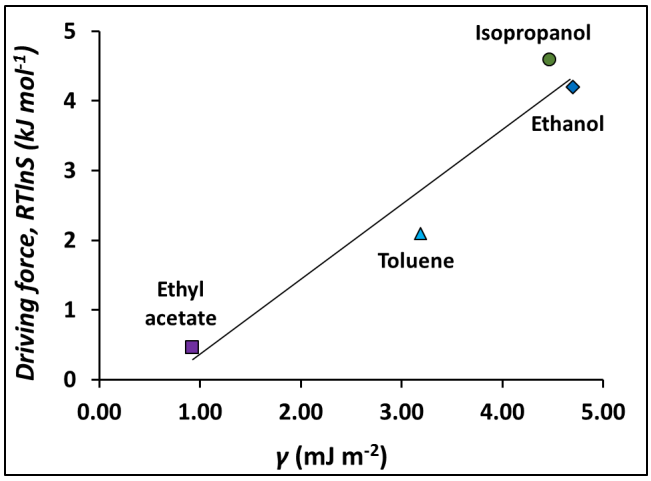

Figure 4: RTlnS required to reach induction times of 4.0 h compared to interfacial energy estimated using CNT.

Quantitatively, γ seems to follow the trend often observed and also predicted using regular solution theory[8] of being inversely proportional to solubility. Unlike other molecules,[9] we found no relation with solvent boiling point. Unexpectedly, we found a strong relationship with solvent density (Supporting Information S3b).

As shown in Table 2, the number of FC molecules in the critical nucleus, n^*, is quite small, ranging from 13 to just under 1. Values approaching unity have recently been found in several similar studies of medium-sized organic molecules,[10, 14, 29] suggesting that CNT appears to underestimate the number of molecules in the critical nucleus.

3.2 FTIR Spectroscopy

Upon heating, fenoxycarb melts at about 54 °C. The FTIR spectra for solid crystalline FC and its melt are shown in Figure 5. In our analysis we focus on the spectral range of 1750-1500 cm^{-1} which owns information about the H-bond sensitive carbonyl ν(C=O) stretching and the amide δ(N-H) bending vibrations. The C=O stretch is peaked in the crystal at 1687 cm^{-1}, and in the melt at 1705-1720 cm^{-1}; this indicates the weakening of interactions of the carbonyl groups in the melt. The amide (N-H) peak which in the crystal is found at 1549 cm^{-1} moves to lower wavenumbers in the melted/disordered state, with the maximum intensity at ca. 1525 cm^{-1}. The observed displacements of the ν(C=O) and δ(N-H) modes upon melting result from the reduction in the C=O…H-N H-bonding present in the FC crystal. The C=C stretching vibration in aromatic rings at ca. 1590 cm^{-1}, and the doublet at 1510 and 1490 cm^{-1}, which originates from the bending vibrations of aromatic and aliphatic C-H groups, are virtually not displaced in going from the crystalline to the melted state.

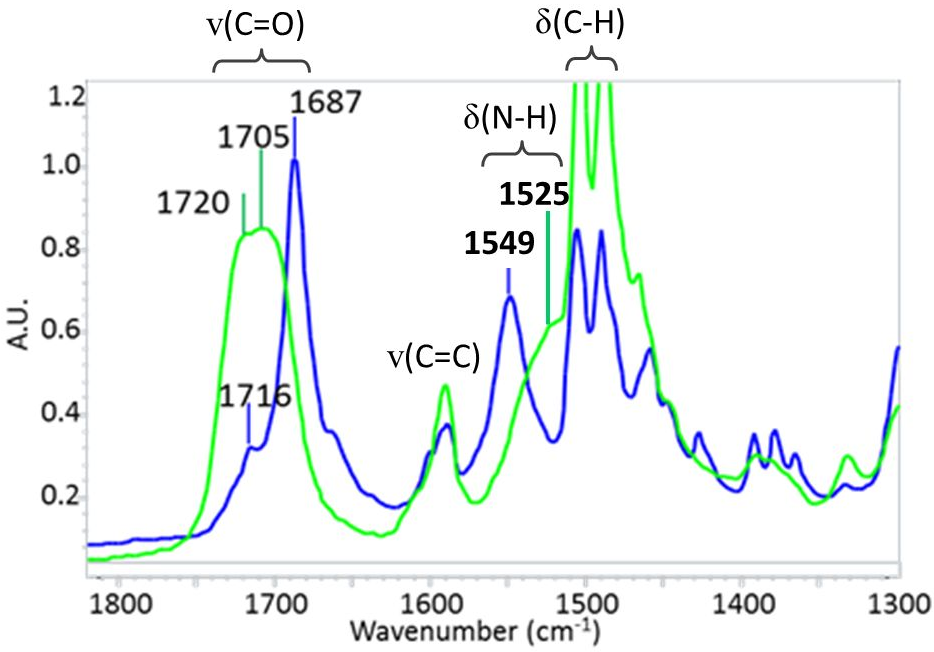

Figure 5: FTIR spectrum of solid fenoxycarb: crystalline (blue) and its melt (green).

During the cooling cycle it was possible to supercool the melt to about 30 °C before it crystallized. No change in the melt spectra from the melting point to 30 °C was observed. The change in the FTIR spectra during heat-cool cycles along with the relevant discussion, are presented in the Supporting Information.

Solution spectra collected for solutions with different concentrations are shown in Figure 6, and the carbonyl stretching frequencies are compared in Table 3. No clear difference appeared between solution spectra in ethanol and isopropanol, and for that reason only isopropanol is shown here.

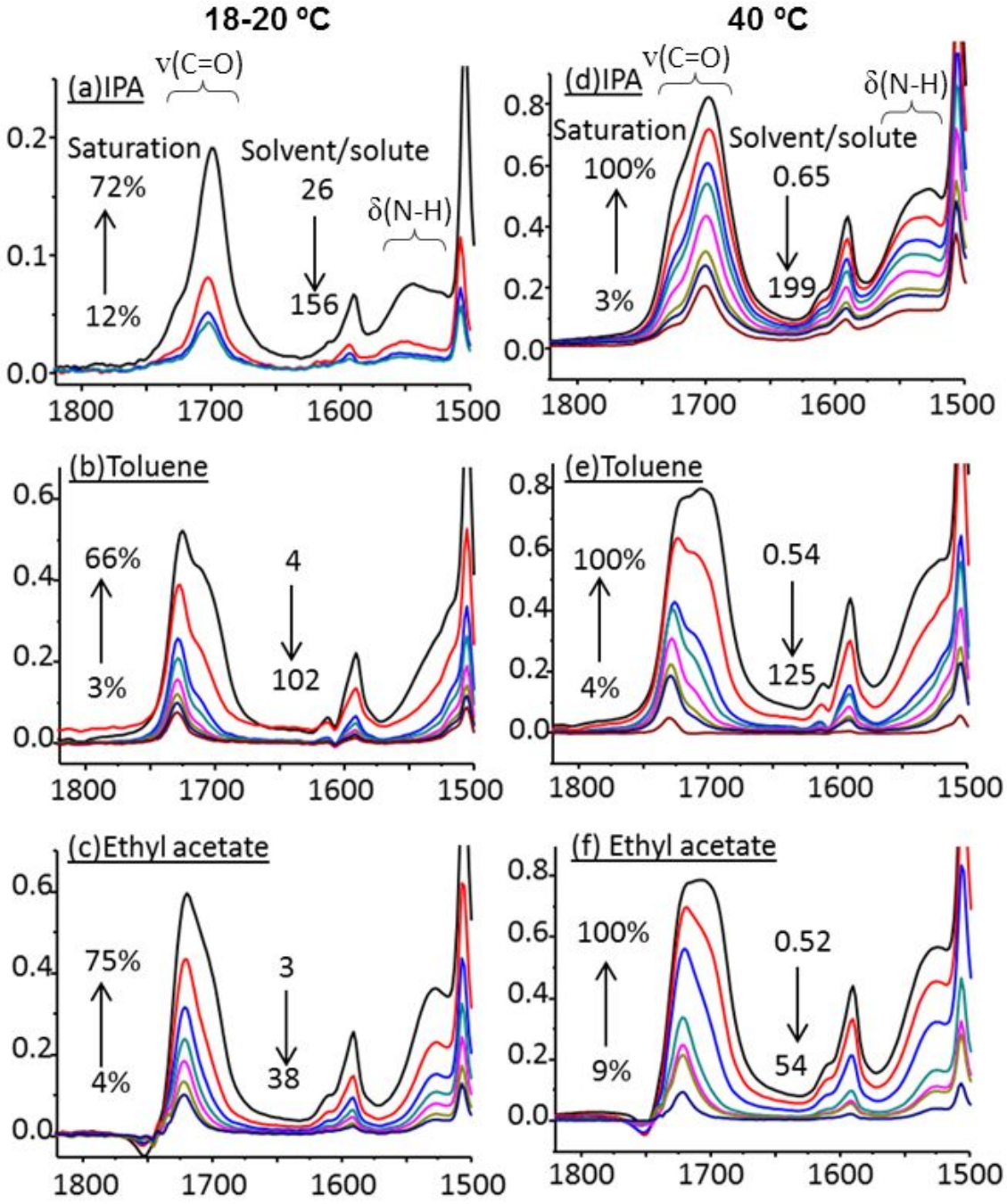

Figure 6: FTIR spectra of FC solutions at room temperature (a, b and c) and 40 °C (d, e and f), saturation and the number of solvent molecules per solute molecule (calculated from the mole fraction concentration) shown for the lowest and the highest concentrations in each case. The solvent spectrum is subtracted from the solution spectra.

Table 3: Summary of the carbonyl stretch ($\nu_{C=O}$) band position (cm^{-1}) at maximum intensity in solution and solid FTIR spectra of fenoxycarb.

Sample	$\nu_{C=O}$ (cm^{-1})	
Solution	dilute (18-20 °C)	concentrated (40 °C)
Toluene	1727	1702
Ethyl acetate	1721	1704
IPA	1702	1700
Solid	crystalline	amorphous (melt)
	1687	1705

The modelled structures, for calculated infrared spectra, are shown in Figure 7 along with their calculated frequencies of the ν(C=O) stretching and δ(N-H) bending vibrations. At first, we compare a single free (not interacting) FC molecule (Figure 7a) with the solid-like cluster of four FC molecules (Figure 7b). To estimate the solvent-related shift of the vibrational modes we have built the models of an FC molecule having its polar groups surrounded/solvated by four molecules of toluene (7c), ethyl acetate (7d) and isopropanol (7e).

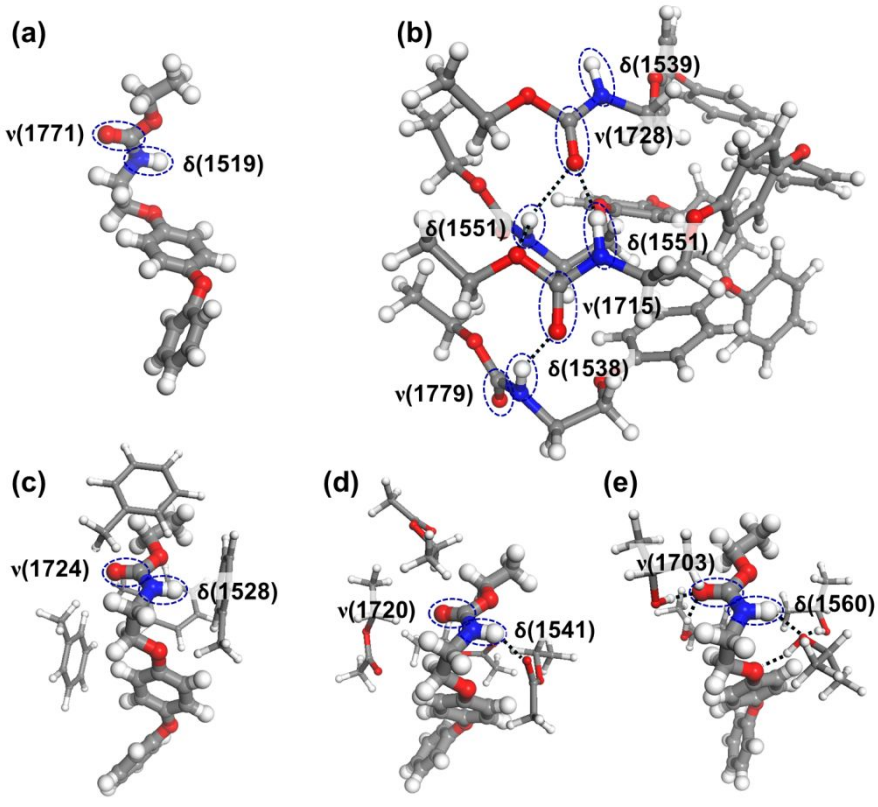

Figure 7: DFT-optimized models along with the ν(C=O) and δ(N-H) simulated infrared vibrational modes (in cm^{-1}) of an isolated (gas-phase) fenoxycarb molecule (a), a cluster of four FC molecules (b), a single FC molecule solvated by four molecules of: toluene (c), ethyl acetate (d), and isopropanol (e). H-bonds shown as dotted black straight lines.

The isolated FC molecule features vibrations of C=O at 1771 cm^{-1} and N-H at 1519 cm^{-1}. In the model of FC solid (Figure 8b) the carbonyl groups involved in H-bonding vibrate at 1715 and 1728 cm^{-1}; this reasonably matches the C=O band of the FC melt (cf. Figure S4, Supporting Information). The different spectral positions of the C=O stretching mode in the different solvents as observed in Figure 6, are related to the strength of interaction of the FC carbonyl group with solvent molecules. The stronger the interaction, the more displaced to lower wavenumbers is the carbonyl band. This feature can be used to rank the strength of the solvent-solute interaction.[13,14] Our solvate models, although simplified, predict the solvent-related shifts of the C=O frequency with a high accuracy (Figures 7c-e). The DFT-calculated vs. experimental ν(C=O) values (at max. intensity) are 1724 and 1727 cm^{-1} (toluene), 1720 and 1721 cm^{-1} (ethyl acetate), and 1703 and 1702 cm^{-1} (isopropanol). Thus, both the experimental and modelling results indicate that the interaction strength of the FC carbonyl with solvent increases in the order: toluene < ethyl acetate < isopropanol.

The δ(N-H) bending vibration shift to 1539 and 1551 cm^{-1} in the solid phase. When interacting with toluene molecules (weak interaction) it shifts to 1528 cm^{-1} and further to 1541 cm^{-1} when H-bonded to the ethyl acetate C=O group (strong interaction) (Figures 7c and 7d). Interestingly, an even more pronounced shift to 1560 cm^{-1} is observed for the FC-isopropanol solvate (Figure 7e), even though the H-bonding strength of alcohol (hydroxyl) oxygen is similar to that of the C=O group of ethyl acetate. The observed strong shift of δ(N-H) predicted in alcohol may originate from the "cooperative effect" of H-bonding. In the alcohol solvate model (Figure 7e) the C=O group of FC is H-bonded to two isopropanol molecules what forces the lone pair of electrons on the nitrogen to delocalize more into the carbonyl. This affects the electron density at the N-H group and yields stronger shift of the N-H mode to higher wavenumbers (see supporting information for relevant examples). This is also observed in the model of FC solid (Figure 8b), where N-H absorbs at a higher wavenumber of 1551 cm^{-1} if the conjugated C=O group is also H-bonded (featuring the chain-like H-bonding as in the FC crystal; this is observed at 1549 cm^{-1} in the crystalline sample, Figure S4, Supporting Information). If the carbonyl group is free (not H-bonded),

then N-H absorbs at 1538 cm^{-1}, even though strongly H-bonded by the carbonyl group of the adjacent FC molecule. The DFT-predicted values of the N-H vibrations of the solvates, though not matching in exact numbers, follow the maximum frequency order of the respective experimental N-H bands of the diluted solutions, i.e. toluene < ethyl acetate < isopropanol (Figure 6).

At ambient temperature (Figure 6, left panel), the dilute solutions of FC prepared in isopropanol, ethyl acetate and toluene show only one dominant peak for carbonyl stretching at 1702, 1721 and 1727 cm^{-1} respectively, in the experimental spectra. With increasing solute concentration in ethyl acetate and toluene, the carbonyl peak shows a shoulder at a lower wavenumber which continually increases with concentration. A rise of this peak at lower frequency in the carbonyl region suggests an increase in strongly bound carbonyl species with increase in the concentration of solute. Interestingly, with increasing concentration this shoulder grows quite rapidly in the case of toluene solutions compared to solutions in ethyl acetate. On the other hand, solutions of isopropanol showed no such concentration effects at room temperature.

In order to investigate the concentration effect for a wider concentration range and to aid interpretation of spectral changes, solution spectra were also collected at 40 °C (Figure 6, right panel). FC is highly soluble in all the solvents at 40 °C, and saturated solutions of FC at this temperature lead to compositions of solutions with less than one molecule of solvent per molecule of solute. Considering the large size of the FC molecule compared to that of the solvent molecules, it is expected that the spectra would reveal structural features from clustering of FC molecules similar to the melt phase. Indeed, the saturated solutions of FC at 40°C in toluene and ethyl acetate show similar spectra to that of the melt (cf. Supporting Information). Furthermore, a similar trend to that observed at room temperature is noticed: with increasing concentration the shoulder at lower wavenumbers increases, which again is more pronounced in toluene. This could be generalized in terms of hydrogen bonding characteristics of these two solvents. Toluene can only weakly interact with a carbonyl group via its C-H hydrogens and it is reasonable that the solute-solute aggregation involving the carbonyl group is more promoted in toluene. Whereas, ethyl acetate is a strong hydrogen bond acceptor and it is expected to interact strongly with the H-bond donating N-H group of FC, thus creating a more effective barrier to solute aggregation.

It is difficult to interpret the solute-solute aggregation information in alcohol solutions as alcohol can act as both hydrogen bond donor and acceptor, which poses difficulty in differentiating solvent-solute and solute-solute interactions. There was no clear concentration effect observed for solutions in alcohols at room temperature. However, at 40 °C, with further increase in concentration, the shoulder at the higher wavenumber increases. This suggests that with decreasing amount of alcohol molecules (increasing concentration of FC), there is also a rise in fraction of the melt-like, relatively loosely bound carbonyl groups of FC molecules.

It should be noted here that the nucleation experiments were carried out in solutions saturated at 15 and 20 °C. It appears from the solution IR spectroscopy that at this temperature the increase in concentration of the ethyl acetate and toluene solutions results in increase in aggregation of strongly bound carbonyl species of FC molecules. On the other hand, the alcohol solutions at room temperature do not show major changes at the carbonyl site with increasing FC concentration. This suggests that the clustering of solute molecules through H-bonding at the C=O site is less developed in the alcohol solvents. The concentration-related clustering of FC molecules clearly observed in ethyl acetate and toluene in the carbonyl region is further evidenced in the amide region. With increasing FC concentration, broadening of the δ(N-H) band towards higher wavenumbers is observed with onset shift from 1525 to 1570 cm^{-1} (in toluene) and from 1540 to 1570 cm^{-1} (in ethyl acetate). In fact, the broadened N-H bands suggest presence of variety of bonding modes, including the strongly interacting crystal-like chains of H-bonds (evidenced at 1549 cm^{-1}), and the melt-like, weakly or non-H-bonding interactions which are suggested to dominate in the melt spectrum at 1525 cm^{-1} (cf. Supporting Information).

3.3 Solution Calorimetry

Experimentally determined enthalpies of solution, $\Delta H_{solution}$, for FC in four different solvents are given in Table 4. Since these values correspond to dissolution of only a small quantity of solute in a large quantity of solvent, the values can be interpreted as essentially being infinite dilution values, $\Delta H^{\infty}_{solution}$. In addition, the table shows calculated values of enthalpy of solvation ($\Delta H_{solvation}$), enthalpy of cavity formation (ΔH_{cavity}) and enthalpy of solvent-solute interactions ($\Delta H_{interaction}$). The ΔH_{cavity} and the related $\Delta H_{interaction}$ values were calculated with both the SPT method and with our alternative approach.

Table 4: Solubility of fenoxycarb in four solvents and enthalpies of solution, solvation, cavity, and interaction, all at 25°C.

Solvent	Solubility (mole fraction)[18]	$\Delta H_{solution}$ (kJ mol^{-1})	$\Delta H_{solvation}$ (kJ mol^{-1})	SPT approach		Alternative approach	
				$\triangle H_{cavity}$ (kJ mol^{-1})	$\triangle H_{interaction}$ (kJ mol^{-1})	$\triangle H_{cavity}$ (kJ mol^{-1})	$\triangle H_{interaction}$ (kJ mol^{-1})
Ethyl Acetate	0.393	24.300 ± 0.063	-146.6	101.1	-246.4	78.1	-224.7
Toluene	0.354	30.477 ± 0.011	-140.5	84.4	-223.2	77.8	-218.3
Ethanol	0.158	32.599 ± 0.106	-138.3	110.6	-247.3	127.0	-265.3
Isopropanol	0.108	38.608 ± 0.009	-132.3	88.5	-219.1	121.0	-253.3

3.4 Computational molecular level analysis

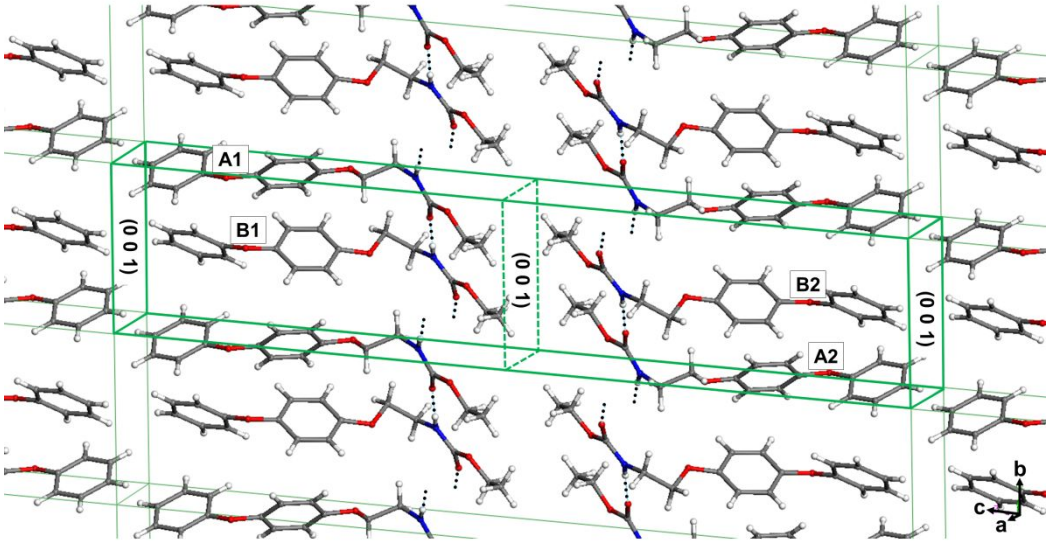

Figure 8: Molecular arrangement in the crystal lattice of FC. Highlighted is a unit cell occupied by four FC molecules having distinct conformations, where A1 – A2 and B1 – B2 are non-superimposable mirror images.

In the FC crystal, there are four distinct molecular conformations, which, in theory, can be interconverted by rotating particular segments around particular single bonds of the FC molecule (Figure 8). We identified three centres of rotation allowing for such an interconversion. The DFT-calculated energy barriers to rotation around those three single bonds are ranging from 5 to 30 kJ mol^{-1} (for details please refer to Supporting Information). Those energy barriers are typical for flexible organic molecules, and according to available experimental data, such barriers should not prevent a molecule from changing conformation in solution.[33] Our computations also indicate that the lowest energy conformations modelled with DFT are very similar to those present in the FC crystal. We did not notice any distinct "wrong" conformations being structurally different (featuring e.g. intramolecular H-bonding) and/or being more stable than those lowest energy crystal-like conformations of the FC molecule.

Examples of clusters extracted from the solutions equilibrated at 2 ºC are shown in Figure 9. FC exhibits very high solubility in ethyl acetate and toluene, and significantly lower, though still relatively high solubility in ethanol and isopropanol. As a result of high solute-to-solvent ratios, clustering of FC molecules is expected in all solvents at the experimental concentrations. This is clearly reflected in our MD simulation snapshots (Figure S5, Supporting Information). At such a high concentration, the computations reveal that the aggregates of FC molecules are largely interconnected and form three-dimensional gel-like structures in ethyl acetate and toluene. In the least concentrated isopropanol solution the clustering is less pronounced, but is still obvious.

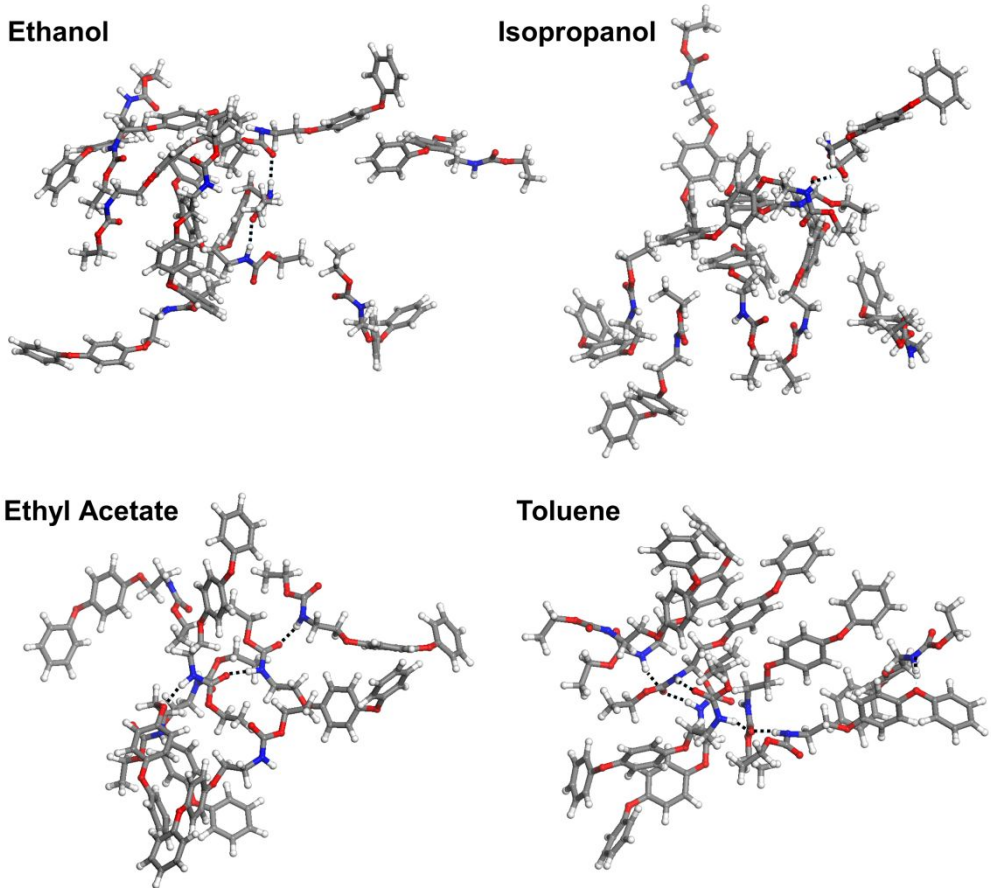

Figure 9: Examples of FC clusters formed at 2 °C in supersaturated solutions of ethanol, isopropanol, ethyl acetate, and toluene. H-bonds are indicated by black dotted lines. Molecules of solvent are not shown. Simulations performed with Molecular Dynamics and a Charmm General Force Field.

The MD simulations confirm the high flexibility of FC molecules. We observe that the FC molecules adapt a variety of conformations in solution, where most geometries are quite different from those of the four crystal lattice conformers. This observation is in line with the relatively low energy barriers to rotation predicted with our DFT computations. It also appears that the molecular geometries/conformations in solution are not specific to the solvent. The clusters (Figure 9) are shown for illustration purposes, as they are transient structures in the constantly changing solution structure. From the comparison of these assemblies it appears that most FC molecules in the clusters formed in ethanol and isopropanol are associated to other FC molecules only by a fraction of their interaction surface, and are, to a great extent, solvated (Figure 9, top). On the other hand, the clusters forming in toluene appears to be more compact, with more pronounced overlapping of the FC molecules.

The MD simulations, regardless of the solvent used, reveal formation in solution of crystal-like H-bonds, (amide)N–H···O=C(carbonyl), and to a lesser extent (amide)N–H···O–C(ether) – the latter not existing in the FC crystal structure. As the former is a feature of the FC crystal, we calculated the radial distribution function (RDF) of interatomic distances of H (amide) and O (carbonyl) between fenoxycarb molecules in the four solvent solutions (Figure 10).

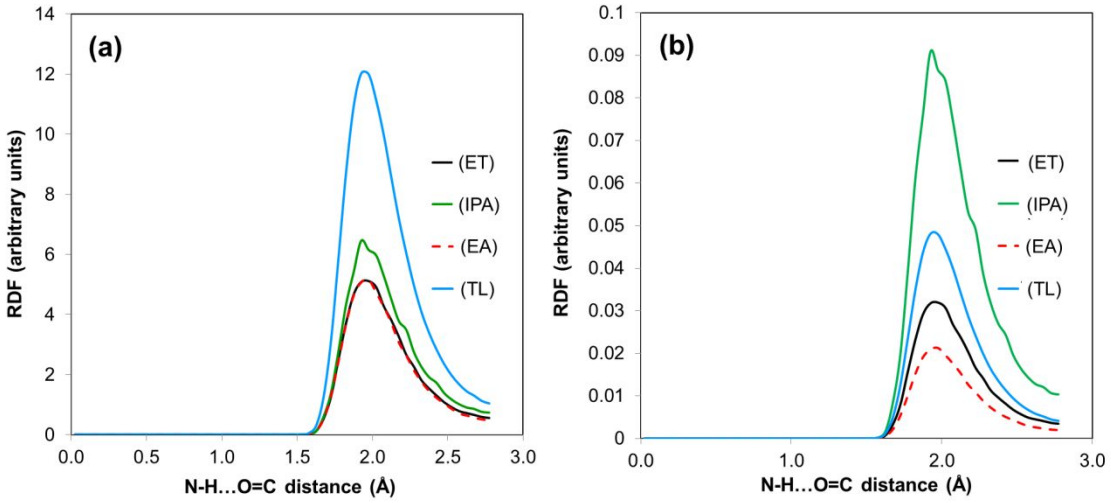

Figure 10: Radial distribution function (RDF) plot for amide hydrogen…carbonyl oxygen hydrogen bonding established by FC molecules in ethanol (ET), isopropanol (IPA), ethyl acetate (ET), and toluene (TL): (a) RDFs calculated for the exact number of fenoxycarb molecules in the simulation boxes, and (b) RDFs normalized per one molecule of FC.

Most of the H (amide) and O (carbonyl) H-bonding appear with a distance of ca. 1.9 Å, i.e. close to that in the crystal (1.95 Å).[15] Figure 10a reveals that the probability of finding the two atoms forming H-bonding is the lowest in ethanol and ethyl acetate, slightly higher in isopropanol and highest in toluene. The high fraction of the N–H···O=C H-bonds observed in toluene can be related to the relatively weak interactions of the toluene molecules with the polar groups of FC. However, the RDF probability depends on the number of solute molecules in the simulation box (which reflect the different concentrations). To account for this, we have normalized the RDFs values per one molecule of fenoxycarb (Figure 10b). The normalized data clarifies that the H-bonding per FC molecule is the lowest in ethyl acetate, then slightly more probable in ethanol. Interestingly, the normalized RDFs suggest that toluene is just at the second place in promoting the H-bonding between FC molecules, being

overtaken by isopropanol. In ethyl acetate the low hydrogen bonding between FC molecules is due to the high affinity of the EA carbonyl group for interaction with the NH group of the solute and in ethanol it is the corresponding action of the ET hydroxyl group.

Our recent work on the nucleation of salicylic acid[13,32], risperidone[14] and tolbutamide[21], suggest that the influence of the solvent on the crystal nucleation is related to the desolvation of the solute molecule. The results suggest that the stronger solvent and solute molecules bind to each other in solution, the more difficult the desolvation, and consequently this slows the nucleation process. To validate this hypothesis further, we have calculated the solvent–solute interaction enthalpies ($\Delta H_{\text{solvent–solute}}$) for both dilute and concentrated solutions of FC (Table 5).

Table 5: Interaction enthalpies (in kJ mol^{-1} ± SD) from molecular dynamics simulations at 2°C of fenoxycarb molecules interacting with bulk solvent (solvent-solute), interactions through clustering of FC molecules in solution (solute-solute), and interactions between solvent molecules in bulk solvent (solvent-solvent).

Interaction type/Solvent	Ethyl acetate	Toluene	Ethanol	Isopropanol
	$\Delta H_{\text{solvent–solute}}$			
Solvent–solute (dilute)[a]	-221.4 ± 15.2	-208.2 ± 13.6	-248.5 ± 23.3	-243.7 ± 23.2
Solvent–solute (concentrated)[b]	-121.8 ± 1.9	-100.6 ± 1.6	-177.7 ± 2.7	-193.6 ± 4.5
	$\Delta H_{\text{solute–solute}}$			
Solute–solute[b]	-204.6 ± 1.2	-216.5 ± 1.2	-181.7 ± 1.6	-168.4 ± 2.5
	$\Delta H_{\text{solvent–solvent}}$			
Solvent–solvent	-71.1 ± 8.2	-71.2 ± 6.2	-84.3 ± 12.9	-91.8 ± 11.8
Solvent–solvent (normalised)[c]	-155.6	-156.3	-253.9	-242.0

[a] A single FC molecule in a box of solvent

[b] Molecular composition of 160 FC + 1848 ET, 71 FC + 1207 IP, 242 FC + 673 EA, and 250 FC + 665 TL

[c] Details of the normalization procedure are presented in Supporting Information

As expected, the solvation enthalpies for the dilute solutions are higher than those of the concentrated solutions regardless of solvent. For the dilute system, the enthalpies reflect binding of one FC molecule placed in a cavity of solvent molecules. In the case of the concentrated solutions, the solute molecules are highly agglomerated, such that certain fractions of strongly binding polar groups are engaged in solute-solute bonding. Thus the solute-solvent binding energies for the concentrated solutions are lower than those for the dilute systems. Lower (less negative) interaction energies of the concentrated solutions indicate more pronounced clustering of the solute molecules. This is corroborated by the calculated solute-solute interaction enthalpies. The results show that toluene and ethyl acetate create an environment where the FC molecules cluster significantly stronger as compared to the solute molecules assembling in ethanol and isopropanol. Our calculations indicate that the solvent-solvent interaction strength is comparable for ethyl acetate and toluene, and is relatively higher for alcohols (Table 5). The interactions of the alcohol molecules being relatively stronger for both the solvent-solvent and the solvent-solute interactions, result in relatively weaker interactions/clustering between the fenoxycarb molecules in the alcoholic solutions (cf. solute-solute values in Table 5).

3.5 Discussion

In this work, the strength of solvent-solute interactions was determined by two different methods: from calorimetrically determined enthalpies of interaction and from the solvent-solute interaction enthalpies derived from the molecular dynamics work. As the experimental and computational approaches both relate to the same physical phenomenon, the calorimetric and MD-calculated enthalpies should cross-validate by showing the same order of the solvent-solute interaction. Indeed the correlation is statistically significant (R^2=0.96, p=0.02) (Figure 11a), and reveals that the solvent-solute interaction increases in the order: toluene < ethyl acetate < isopropanol < ethanol. Furthermore, both the calorimetric and computational results show a consistent relationship with the IR carbonyl stretching peak position that reflects the strength in the solvent-solute binding at this site (Figure 11b). Thus, the interaction order obtained from calorimetric, MD calculations (dilute solutions) and spectroscopic data (for the C=O site) all agree on the order among the solvents with respect to the strength of solvent-solute interactions (Figure 11 (a) and (b)). In case of MD calculations for concentrated solutions, the order of the alcohols is reversed as compared to the dilute solutions and in case of spectroscopic data it was difficult to differentiate the shifts between

the two alcohols. However, overall the results give evidence of the validity of all three methods as measurements for the strength of the solvent-solute interactions.

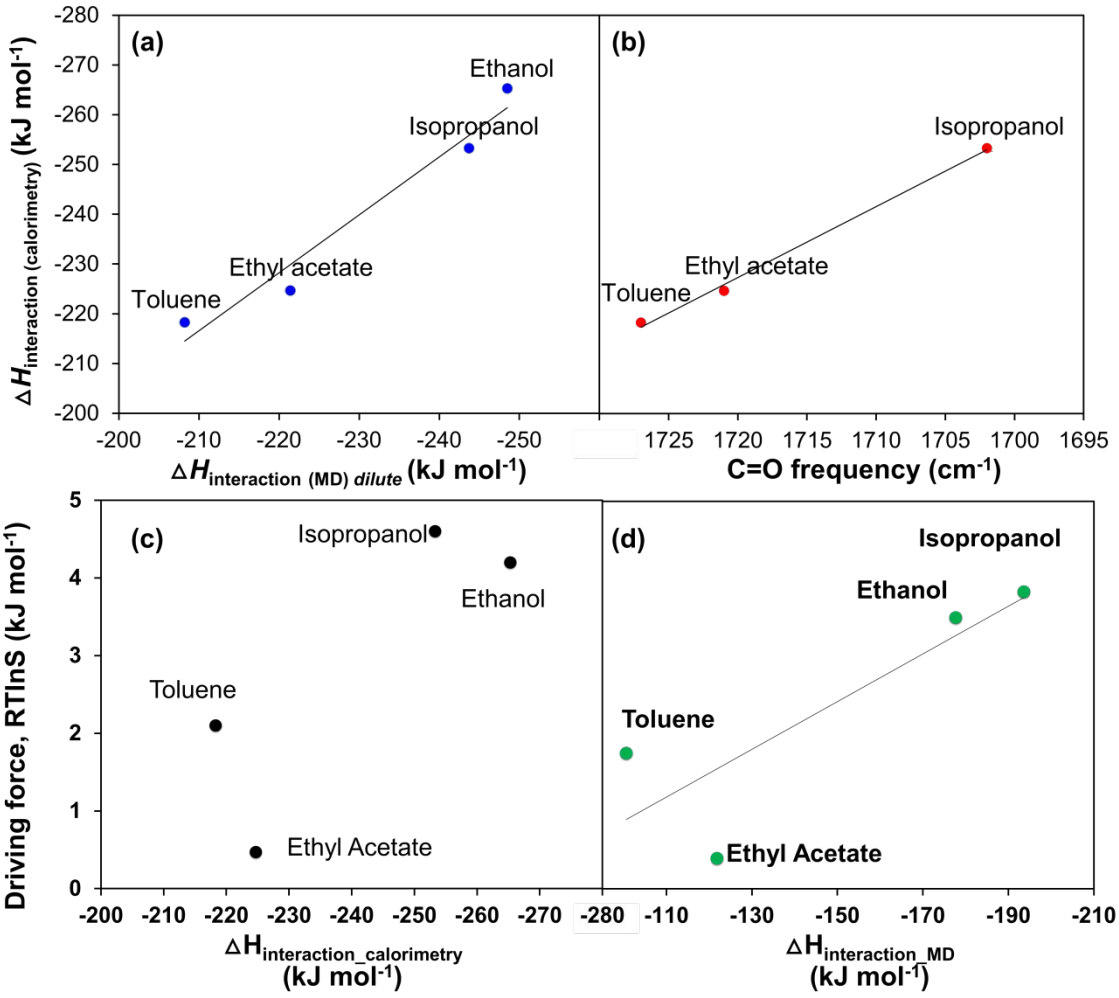

Figure 11: Relationship between the calorimetric solvent-solute interaction enthalpy of FC in four different solvents and (a) MD-calculated solvent-solute interaction enthalpy (dilute solutions) and (b) FTIR frequency of the fenoxycarb carbonyl band in diluted solutions. Comparison of driving force, RTLnS, at median induction time of 4.0 h with (c) calorimetric interaction enthalpy and (d) MD-calculated solvent-solute interaction enthalpy (concentrated solutions) is given.

Table 6: Difficulty of nucleation and strength of solvent-solute interaction

Solvent	Ease of Nucleation	Solvent-Solute Interaction

	RTlnS for t_{ind} = 4.0 h (kJ/mol)	γ (mJ m^{-2})	Calorimetric $\triangle H_{interaction}$ (kJ mol^{-1})	Spectroscopic C=O (cm^{-1})	MD dilute $\triangle H_{interaction}$ (kJ mol^{-1})	MD conc. $\triangle H_{interaction}$ (kJ mol^{-1})
Ethyl Acetate	1	1	2	2	2	2
Toluene	2	2	1	1	1	1
Ethanol	3	4	4	4	4	3
Isopropanol	4	3	3	3	3	4

In recent work on salicylic acid and risperidone we found that nucleation from different organic solvents became more difficult as the solvent-solute interactions became stronger.[13, 14] This was based on similar nucleation, spectroscopic, calorimetric and modelling work.The relationship was rationalised by the hypothesis that the stronger the solvent binds the solute, the more difficult the nucleation becomes, and points to the importance of desolvation in the formation of a nucleus.

Nucleation of FC in the four solvents investigated shows overall a similar trend (cf. Figure 11 (c) and (d), and Table 6). Compared to the alcohols, toluene and ethyl acetate have weaker solvent-solute interactions with FC and accordingly nucleation is more easy (i.e. lower γ and lower RTlnS at median t_{ind} = 4.0 h).

Besides the apparent differences in the solvent-solute interactions, the solubility mole fraction is clearly higher in toluene and ethyl acetate, as compared to ethanol and isopropanol. As observed in our MD simulations, the higher concentration of the FC molecules in toluene and ethyl acetate facilitates their clustering more than in the alcoholic solutions. Thus, besides the lower energy barriers to desolvation, as indicated by the lower solvent-solute interactions, the nucleation of fenoxycarb in toluene and ethyl acetate appears to be also promoted by the relatively higher concentration of the solute molecules. The exact order between isopropanol and ethanol, with respect to both ease of nucleation and solvent-solute interaction, is somewhat ambiguous since they are close, with different measurement methods giving slightly different orders (e.g. ethanol has a slightly higher γ than isopropanol but a slightly lower *RTlnS*).

The discrepancy between ethyl acetate and toluene is somewhat more significant; despite having a slightly weaker solvent-solute interaction than ethyl acetate, it is more difficult to

nucleate from toluene. In our work on risperidone, toluene fits well into the overall trend of easier nucleation being related to weaker solvent-solute interactions.[14] However, for tolbutamide[21] we also observe that nucleation is relatively difficult from toluene despite relatively weak solvent-solute interactions. However, by employing molecular dynamics we predicted that in toluene the tolbutamide molecule tends to adopt an intramolecularly hydrogen bonded conformation, substantially different from and more stable than the conformation in its crystal structure. Thus we concluded that the experimentally observed very difficult nucleation of TB in toluene can be rationalised by the preferential formation of the crystal-incompatible conformation. In the present work however the DFT conformational analysis conducted has indicated neither "wrong" conformation(s) nor high rotational barriers for interconversion between the crystal-like conformations of fenoxycarb. It should be noticed that those rotational energy barriers were calculated in a gas-phase, thus without considering the solvent influence on the barrier height. It is therefore possible that when considering a particular solvent environment, the potential energy landscape may be quite different from that calculated for the gas-phase FC molecule.

The question remains: why fenoxycarb nucleated from toluene does not follow the desolvation difficulty rule observed for salicylic acid and risperidone? A distinct feature of toluene, as compared to the other solvents studied, is lack of a propensity for strong H-bonding with solute molecules. This leads to the most pronounced clustering of FC molecules in toluene as predicted with our MD simulations and observed with FTIR spectroscopy. Although more clustering of solute could indicate easier nucleation, our results suggest that those prenucleation clusters formed in toluene do not easily turn into crystalline particles. One reason could be the formation in those molecular aggregates a network of H-bonds featuring interactions being different from the H-bonds present in the FC crystal, such as e.g. (amide)N–H···O–C(ether). This could be associated with substantially different orientations and conformations of the FC molecules within clusters of solute forming in toluene.

Despite some inconsistencies, we believe the overall trend of stronger solvent-solute binding leading to more difficult nucleation is also generally observable in the case of FC. Compared to in alcohols, FC is easier to nucleate from toluene and ethyl acetate, and has lower solvent-solute interaction energies with them. However, evidence is mounting that it is too simplistic to believe that the strength in solvent-solute interactions can provide for a full explanation of the nucleation of more complex molecules in different solvents.

4 Conclusion

Crystal nucleation of fenoxycarb in different solvents becomes gradually more difficult in the order ethyl acetate, toluene, ethanol and isopropanol, with only a relatively minor difference between the alcohols. This is in good agreement with the order of increasing interfacial energy determined within the classical nucleation theory. This influence of the solvent on the nucleation is reasonably well captured by the relative prominence of solvent-solute interactions as determined from spectroscopic, calorimetric and molecular dynamics investigations. The stronger the binding of the solvent to the solute the more difficult the nucleation becomes. An exception to this trend is toluene, which despite having the weakest solvent-solute interaction exhibits medium nucleation difficulty.

Supporting Information

The details of the experimental and computational porcedures, results of the conformational analysis, the temperature-dependent time-resolved FTIR spectroscopy and statistical analysis are shown in the Supporting Information file.

Acknowledgements

The financial support of Science Foundation Ireland (SFI, grant numbers 10/IN.1/B3038 and 11/SIRG/B2111), and of the Swedish Research Council (621-2010-5391) and the donation of fenoxycarb material by Syngenta, Switzerland are gratefully acknowledged. J. Zeglinski acknowledges the SFI and Higher Education Authority funded Irish Centre for High End Computing for access to computational facilities. A. Hegarty wishes to acknowledge the support of the Mathematics Applications Consortium for Science and Industry (www.macsi.ul.ie) funded by the Science Foundation Ireland Investigator Award 12/IA/1683.

Bibliography

(1) Valder, C.; Merrifield, D., *Pharmaceutical Technology*. SmithKline Beecham R&D News **1996,** 32.

(2) Bernstein, J., *Polymorphism in Molecular Crystals*. Ed.; Oxford University Press: Oxford, **2002**.

(3) Leng, J.; Salmon, J.-B., Microfluidic crystallization. *Lab Chip* **2009,** 9, 24-34.

(4) Rodríguez-hornedo, N.; Murphy, D., Significance of controlling crystallization mechanisms and kinetics in pharmaceutical systems. *J. Pharm. Sci.* **1999,** 88, 651-660.

(5) Vekilov, P. G., Nucleation. *Cryst. Growth Des.* **2010,** 10, 5007-5019.

(6) Revalor, E.; Hammadi, Z.; Astier, J.-P.; Grossier, R.; Garcia, E.; Hoff, C.; Furuta, K.; Okustu, T.; Morin, R.; Veesler, S., Usual and unusual crystallization from solution. *J. Cryst. Growth* **2010,** 312, 939-946.

(7) Ostwald, W. Z., Studies on the formation and transformation of solid compounds: Report I. Supersaturation and practicing cooling. *Z. physik. Ch.* **1897,** 22, 289-330.

(8) Mullin, J. W., *Crystallization, Fourth Edition*. Ed.; Butterworth-Heinemann: 2001.

(9) Yang, H.; Rasmuson, Å. C., Nucleation of Butyl Paraben in Different Solvents. *Cryst. Growth Des.* **2013,** 13, 4226-4238.

(10) Yang, H.; Svärd, M.; Zeglinski, J.; Rasmuson, Å. C., Influence of Solvent and Solid-State Structure on Nucleation of Parabens. *Cryst. Growth Des.* **2014**, 14, 3890-3902.

(11) Kuhs, M.; Zeglinski, J.; Rasmuson, Å. C., Influence of History of Solution in Crystal Nucleation of Fenoxycarb: Kinetics and Mechanisms. *Cryst. Growth Des.* **2014**, 14, 905-915.

(12) Gracin, S.; Rasmuson, Å. C., Polymorphism and Crystallization of p-Aminobenzoic Acid. *Cryst. Growth Des.* **2004,** 4, 1013-1023.

(13) Khamar, D.; Zeglinski, J.; Mealey, D.; Rasmuson, Å. C., Investigating the role of solvent-solute interaction in crystal nucleation of salicylic acid from organic solvents. *J. Am. Chem. Soc.* **2014**, 136, 11664-11673.

(14) Mealey, D.; Zeglinski, J.; Khamar, D.; Rasmuson, A., Influence of Solvent on Crystal Nucleation of Risperidone. *Faraday Discuss.* **2015**, 179, 309-328.

(15) Karpinska, J.; Kuhs, M.; Rasmuson, A.; Erxleben, A.; McArdle, P., Ethyl N-[2-(4-phenoxyphenoxy)ethyl]carbamate. *Acta Crystallogr. E* **2012,** 68, 2834-2835.

(16) Masner, P.; Angst, M.; Dorn, S., Fenoxycarb, an insect growth regulator with juvenile hormone activity: A candidate for Heliothis virescens (F.) control on cotton. *Pestic. Sci.* **1987,** 18, 89-94.

(17) Xiao-Hong, S.; Yuan-Fa, L.; Zhi-Cheng, T.; Ying-Qi, J.; Jian-Wu, Y.; Mei-Han, W., Heat Capacity and Enthalpy of Fusion of Fenoxycarb. *Chin. J. Chem.* **2005,** 23, 501-505.

(18) Kuhs, M.; Svärd, M.; Rasmuson, Å. C., Thermodynamics of fenoxycarb in solution. *J. Chem. Thermodyn.* **2013,** 66, 50-58.

(19) Zeglinski, J.; Svard, M.; Karpinska, J.; Kuhs, M.; Rasmuson, A., Analysis of the structure and morphology of fenoxycarb crystals. *J. Mol. Graph. Model.* **2014**, 53, 92-99.

(20) Ouvrard. C.; Mitchell, J. B. O., Can we predict lattice energy from molecular structure? *Acta Crystallogr. B* **2003**, B59, 676-685.

(21) Zeglinski, J.; Kuhs, M.; Khamar, D.; Hegarty, A. C.; Devi, R. K.; Rasmuson, Å. C., Crystal Nucleation of Tolbutamide in Solution: Relationship to Solvent, Solute Conformation, and Solution Structure. *Chem. Eur. J.* **2018**, 24, 4916-4926.

(22) Morel-Desrosiers, N.; Morel, J.-P., Evaluation of thermodynamic functions relative to cavity formation in liquids: uses and misuses of Scaled Particle Theory. *Can. J. Chem.* **1981**, 59, 1-7.

(23) Grimme, S.; Ehrlich, S.; Goerigk, L., Effect of the damping function in dispersion corrected density functional theory. *J. Comput. Chem.* **2011**, 32, 1456-1465.

(24) Rassolov, V. A.; Ratner, M. A.; Pople, J. A.; Redfern, P. C.; Curtiss, L. A., 6-31G* Basis Set for Third-Row Atoms. *J. Comput. Chem.* **2001**, 22, 976-984.

(25) Frisch, M. J.; Trucks, G. W.; Schlegel, H. B.; Scuseria, G. E.; Robb, M. A.; Cheeseman, J. R. et al., *Gaussian 09*, Revision D.01, Gaussian Inc., Wallingford, CT, **2013**.

(26) Phillips, J. C.; Braun, R.; Wang, W.; Gumbart, J.; Tajkhorshid, E.; Villa, E. et al., Scalable molecular dynamics with NAMD. *J. Comput. Chem.* **2005**, 26,1781-1802.

(27) Humphrey, W.; Dalke, A.; Schulten, K., VMD - Visual Molecular Dynamics. *J. Mol. Graph.* **1996**, 14, 33-38.

(28) Vanommeslaeghe, K.; Hatcher, E.; Acharya, C.; Kundu, S.; Zhong, S.; Shim, J. et al., CHARMM general force field: A force field for drug-like molecules compatible with the CHARMM all-atom additive biological force fields. *J. Comput. Chem.* **2010**, 31, 671–690.

(29) Kalbfleisch, J. D.; Prentice, R. L., *The Statistical Analysis of Failure Time Data*. John Wiley & Sons, **2011**.

(30) Petrie, A.; Sabin, C., *Medical Statistics at a Glance*. John Wiley & Sons, **2009**.

(31) Cox, D. R., Regression Models and Life-Tables. *J. R. Stat. Soc. Series B* **1972**, 34, 187-220.

(32) Mealey, D.; Croker, D. M.; Rasmuson, A., Crystal nucleation of salicylic acid in organic solvents. *CrystEngComm* **2015**, 17, 3961-3973.

(33) Derdour, L.; Pack, S. K.; Skliar, D.; Lai, C. J.; Kiang, S., Crystallization from solutions containing multiple conformers: A new modeling approach for solubility and supersaturation. *Chem. Eng. Sci.* **2011,** 66, 88-102.

For Table of Contents Use Only

Probing Crystal Nucleation of Fenoxycarb from Solution through the effect of Solvent

Jacek Zeglinski, Manuel Kuhs, K. Renuka Devi, Dikshitkumar Khamar, Avril C. Hegarty, Damien Thompson and Åke C. Rasmuson

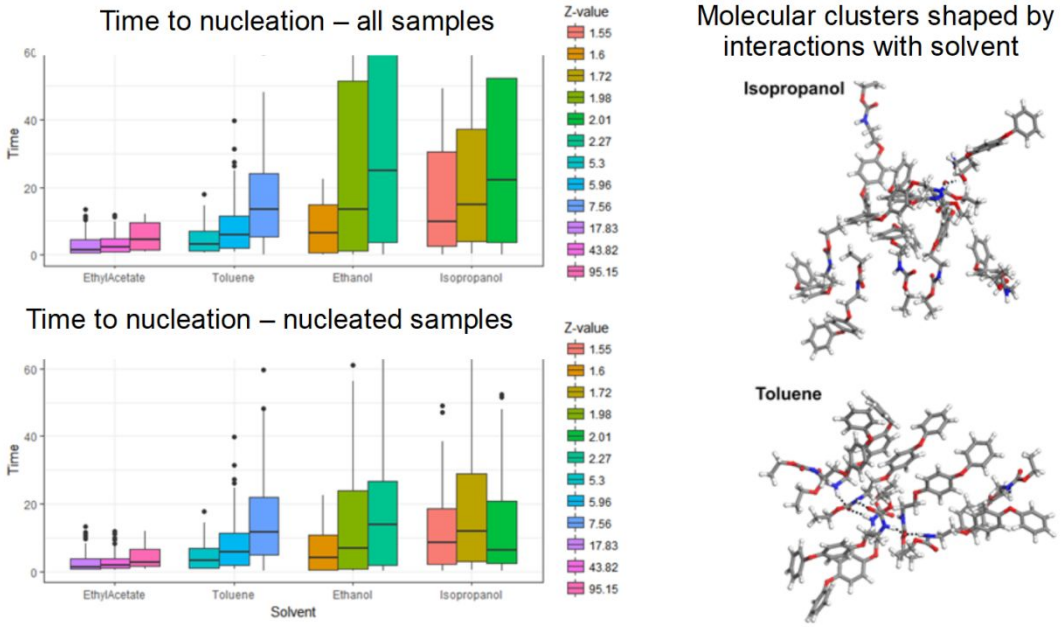

Synopsis

This work includes determination of nucleation induction times of fenoxycarb (a medium-sized flexible drug-like molecule) in four different solvents, estimation of the solvent–solute interaction strength via solution calorimetry, FTIR spectroscopy, and molecular dynamics simulations, and computational investigation of molecular conformations and clustering. In addition, survival analysis is employed to test the significance of effects of the solvents and the nucleation driving force parameters.